

Triggering flow of jammed cohesive granular materials using modulated pulsed airflow

Lizhuo Zhu | Haifeng Lu | Xiaolei Guo | Haifeng Liu

Shanghai Engineering Research Center of Coal Gasification, East China University of Science and Technology, Shanghai, China

Correspondence

Haifeng Lu and Haifeng Liu, Shanghai Engineering Research Center of Coal Gasification, East China University of Science and Technology, P. O. Box 272, Shanghai 200237, China.
Email: luhf@ecust.edu.cn and hflu@ecust.edu.cn

Funding information

National Key R&D Program of China, Grant/Award Number: 2018YFC0808500; National Natural Science Foundation of China, Grant/Award Number: 51876066; Shanghai Engineering Research Center of Coal Gasification, Grant/Award Number: 18DZ2283900

Abstract

Realizing the stable high-flux flow of cohesive granular materials is a complicated subject. We experimentally studied the dynamic characteristics of cohesive granular materials discharged from hopper under modulated pulsed airflow. Results show that pulsed airflow with a smaller duty cycle can effectively trigger the stable flow of jammed cohesive granular materials. Furthermore, under proper working conditions, the hopper flow will change from the classic arch breaking mode to a free flowing mode like liquid. The flow rate of the powder in the free flowing mode will decrease as powder bed height decreases, which overturns the consistent recognition. The oscillating shear provided by the pulsed airflow eliminates the Janssen effect and achieves a liquid-like stress transmission, which supports the above findings. Through energy analysis, we gave the scaling relationship between the pressure gradient and the pulse parameters to cover the experimental data and revealed the internal mechanism.

KEYWORDS

cohesive powders, granular flow, hopper discharge, pulsed airflow, stress transmission

1 | INTRODUCTION

Granular materials are widely found in nature.¹ Many process materials, intermediates or products in the chemical industry exist in the form of powder.² Due to its strong agglomeration and unpredictable flow properties, cohesive powder poses a major challenge to its handling and transportation process.³ Granular systems are discrete and dissipative, therefore exhibit a variety of dynamics.^{4,5} As the particle size decreases, particles will exhibit many peculiar and useful properties, and the field of materials is developing toward the micro-nano scale.⁶ However, for fine cohesive granular materials, the interparticle force cannot be ignored compared to its gravity and is dominant in controlling particle motion, which will show strong agglomeration, poor fluidity, and complex dynamic behaviors.⁷⁻⁹ This poses a challenge to the handling and transportation of granular materials. How to reduce the cohesive force and make granular materials have excellent fluidity like liquids is an interesting and valuable subject both in science and engineering.

External shear will change the local packing fraction and micro-topological structure of particles, thereby affecting granular flow dynamics.¹⁰⁻¹² And recent works have focused on exploring the

effect of dynamic load on the mechanical response of granular materials, relevant to rheology,¹³⁻¹⁷ instability,¹⁸⁻²¹ and friction suppression.²²⁻²⁷ Vibration plays a key role in the friction suppression of the particle system, and the mechanism is believed to be that the vibration reduces the effective interface contact of the particles.²² It is used to provide perturbation and energy to destabilize the arch in silo, thereby trigger flow.²⁸⁻³⁰ Simulation studies have shown that it is possible to control global mobility by applying horizontal or vertical periodic perturbation inside the disordered particle system.³¹ Recent study clearly gave the experimental results of controlling viscosity of dense granular materials through vertical vibration, and further analyzed the mechanism of viscosity reduction and recovery based on collision and dissipation.¹³ However, the introduction of mechanical vibration is usually very energy intensive and not effective enough in large systems. In contrast, pulsed airflow is a simple and effective method to transmit dynamic perturbances to particles.³² Acoustic field is also a way to provide dynamic load and input energy to granular materials. The formation of acoustic oscillation inside the system can lower the friction threshold of the granular system,^{25,33} soften the stress system,^{34,35} and promote the entire fluidization.²³ Aeration is an

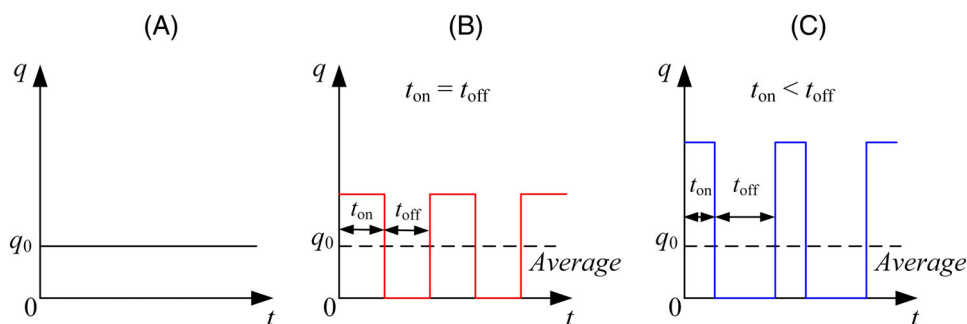


FIGURE 1 Schematic diagram of airflow waveform. (A) steady airflow, (B) square-wave pulsed airflow, (C) modulated pulsed airflow

effective method widely used in promoting the flow of cohesive powders.^{36–38} The fluidization of particles by gas is considered to be an effective means to improve flowability.³⁷ For highly cohesive powders, it is difficult to fluidize due to the prone to channeling. Vibrated fluidization was introduced as a process intensification method.^{39–42} This approach is effective in breaking agglomerates and improving the quality of fluidization. Recent theoretical study has pointed out that the existence of oscillatory instability mechanism inside the granular medium provides a basis for the exponential growth of perturbances and triggering macroscopic collapse and failure.¹⁹ External field excitation is an effective strategy for regulating dynamic characteristics of granular materials. Here, we are interested in whether it can be applied to overcome the cohesive force between particles, thereby triggering stable flows.

The method commonly used to promote the flow of granular materials is to introduce a stable airflow (Figure 1(A)), but this method has limited effects on those with strong cohesion. Moreover, the pulsed airflow provides both oscillating shear and drag force to cohesive granular materials. In our previous work, we studied the effect of square-wave pulsed airflow on the avalanche of cohesive granular materials,⁴³ as shown in Figure 1(B). But for cohesive particles, when the superficial gas velocity beyond the terminal velocity, the particles will be taken out of the bed. In this work, a new method using low duty cycle rectangular pulse flow was proposed, as shown in Figure 1(C). This method can improve the instantaneous gas velocity by reducing the pulse duty cycle while the apparent gas velocity remains unchanged, thus providing a stronger instantaneous pulse aerodynamic force.

In this work, we report that jammed cohesive granular materials driven by a low duty cycle pulsed airflow can discharge from hopper with stable high-flux. We observed the transition of granular hopper flow from arch breaking mode with a low flow rate to free flowing mode with a high flow rate. Moreover, the mechanism of this transition is explained through the characteristics of stress transmission, and the dispersion relationship between the pulsed airflow parameters and discharge rate is also given.

2 | EXPERIMENTAL METHODS

2.1 | Materials

The alumina powder with diameter $d_{32} = 4.6 \mu\text{m}$ and bulk density $\rho_b = 521 \text{ kg/m}^3$ was used as experimental media. The particle size

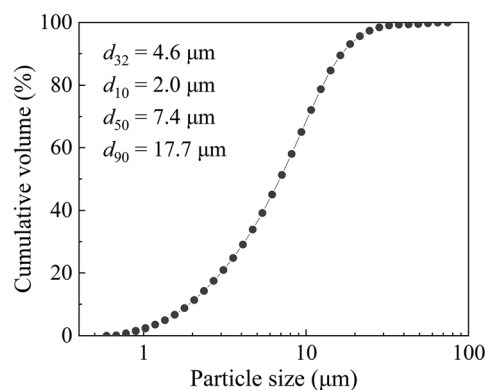


FIGURE 2 Cumulative particle size distribution of the alumina powder

distribution was measured using a Malvern Mastersizer 2000 with a wet dispersion unit (Malvern Instruments). The cumulative particle size distribution was shown in Figure 2. Bulk density was measured by the powder tester PT-X (Hosokawa Micron Corporation). The shear tests were carried out using the rotational shear cell accessory of the FT4 powder rheometer (Freeman Technology). The powder sample is first processed into a loose state. Then slowly precompact with the ventilated piston to slowly precompact under a certain normal stress (3, 6, 9 kPa). The shear head applies a specified normal stress to the powder bed and starts to rotate to induce shear stress. When the powder bed fails, the value of the critical shear stress is recorded. The detailed experimental procedures can be found in Reference.44 Further, using Mohr's circle theory, the powder flow properties including major principal stress (σ_1), unconfined yield stress (f_c), cohesion (C), and angle of internal friction (ϕ) can be obtained and the results was shown in Figure 3. The cohesion C represents the cohesion between particles, the unconfined yield stress f_c represents the consolidation strength of the bed, and the internal friction angle ϕ represents the friction properties. The powder has a flow function (ff_c) in the range of 2–4, which is a typical cohesive powder according to the Jenike flow function criteria.⁴⁵

2.2 | Aerated discharge system

Figure 4 illustrates the experimental setup. The experimental system consists of a pulsed airflow path and a lab scale Plexiglass

hopper. The hopper half angle is $\alpha = 15^\circ$ and the height of aeration vents from the outlet is 60 mm. Four aeration vents with internal diameter of 10 mm were mounted to the produce jets normal to the conical hopper wall. The internal diameter of cylindrical bin is 150 mm and the internal diameter of outlet is 20 mm. These structural parameters are determined by previous research results,⁴⁶ which is more favorable to promote cohesive powders flow. Dry compressed air was used as gaseous media. A flowmeter was used to adjust air rate. The

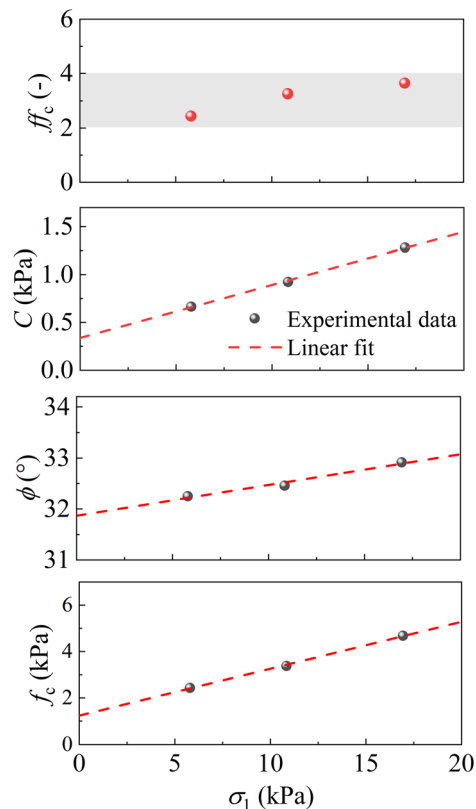


FIGURE 3 Shear test results of the alumina powder, including flow function (ff_c), cohesion (C), internal friction (ϕ), and unconfined yield stress (f_c)

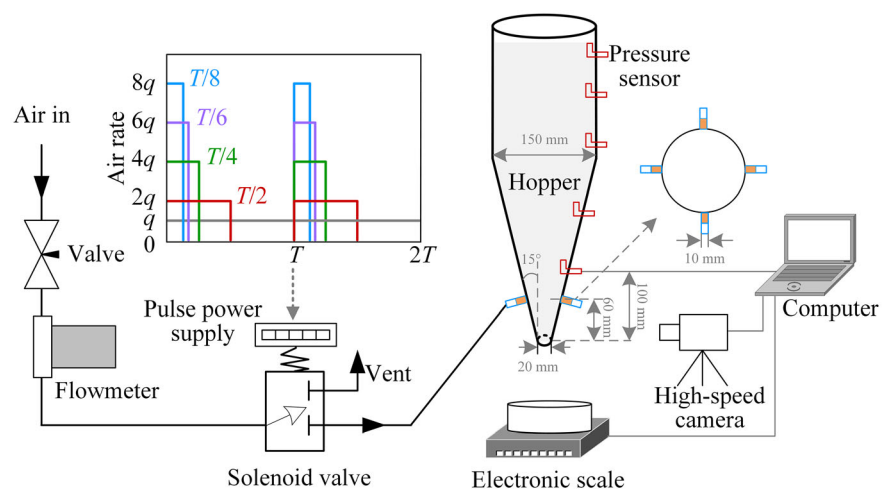
hopper is fixed on an all-metal frame and grounded to eliminate the effects of electrostatic charges. The powder was stored in the hopper, and then rectangular pulsed airflow was aerated in the hopper to trigger flow. An electronic scale (YZ, AWH-10) was used to record the weighing signal and calculate the discharge rate W of powders. A high-speed camera (Phorton, Fstcam SA2) was used to record oscillation motion of granular packing and discharge flow characteristics. A set of pressure sensors (the height from the outlet of 10, 20, 30, 40, 45 cm) were used to record pressure signals during packing and flow. The pressure sensor used in the experiment is diaphragm type, which measures a combination of the gas and solid pressure.^{47,48}

The pulsed airflow was generated by a solenoid valve (Festo, MHE3-MS1H) driven by rectangular pulse power supply. The frequency f (range 0–50 Hz) and duty cycle D (range 1/8–1) of the rectangular wave pulse current can be adjusted to generate a rectangular pulse air flow with designed parameters. The duty cycle is defined as the proportion of the valve opening time relative to the total time in one pulse period, namely $D = t_{on}/T$, where t_{on} is the valve opening time and T is the time of a single period. When adjusting the duty cycle of the pulse waveform, the air rate q will be adjusted by the corresponding multiple to ensure that the average volume is consistent, as shown in Figure 4. For smaller D , the pulsed airflow has higher instantaneous kinetic energy. The air rate q mentioned in the following refers to the average value of the gas entering the hopper in a single period. The influence of pulsed airflow waveform parameters on the discharge flow characteristics of powders was investigated. Experiments for each working condition were repeated more than three runs to ensure reproducibility, and the discharge rate represents an average value.

2.3 | Fluidization test

Fluidization test was carried out on the FT4 powder rheometer. A glass cylinder with an inner diameter of 50 mm was used as the fluidized column. A sintered porous metal plate was inserted at the bottom of cylinder as a gas distributor. Through the customized test

FIGURE 4 Sketch of experimental setup. The inserted rectangular block diagram shows the modulation method of pulsed airflow



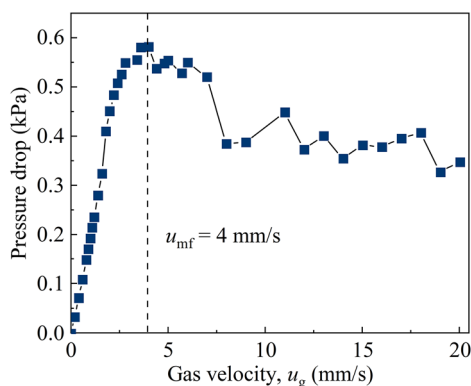


FIGURE 5 Fluidization curve of the alumina powder

program, the gas velocity entering the fluidized column can be adjusted and the bed pressure drop can be recorded. Before the fluidization test, the superficial gas velocity of 40 mm/s is used to make the bed bubbling fluidized to eliminate the memory of the bed structure. The fluidized curve is shown in Figure 5. The minimum fluidization gas velocity u_{mf} is 4 mm/s. Taking the cross section of the cylindrical part of the silo as the flow area, the minimum fluidization air rate is $q_{mf} = 4.24$ L/min.

3 | RESULTS AND DISCUSSION

3.1 | Flow pattern transition

The alumina powder with strong cohesive force and high unconfined yield strength cannot be discharged from the hopper without aeration. The excitation of pulsed airflow can trigger the jammed granular materials flow out from the hopper. Two flow patterns were observed at different aeration rates and pulse waveforms: arch breaking and free flowing. The select snapshots are shown in Figure 6(A), (B). Arch breaking is a typical phenomenon in hopper flow,^{49,50} in which arches sporadic apparition above the outlet of the hopper, as shown in Figure 6(A). It is a persistent sable arch accompanied by the breaking and falling of materials. The discharge rate fluctuates with the sporadic apparition. In this mode, the average discharge rate is controlled by the frequency and amount of arch collapse, and the discharge rate is constant and independent with the upper packing depth. When the duty cycle of the pulsed airflow is reduced, the higher instantaneous kinetic energy of the pulsed airflow provides a strong impact to the powder in the silo. The free flowing mode appeared. As can be seen in Figure 6(B), for free flowing, the material flows out uniformly and continuously from the hopper without the formation of arches. In this mode, the average outflow velocity is significantly higher than that of arch breaking. And the outflow velocity decreases with the decrease of the upper packing depth. Figure 6(C) shows the comparison of time series of outflow velocity of pseudo ideal fluid, water, glycerine, and alumina in two flow patterns. The pseudo ideal fluid here assumes a

medium that has the same bulk density as alumina but satisfies the assumption that the fluid is continuous and non-viscous. When it flows, the potential energy is completely converted into kinetic energy, and there is no energy dissipation. The outflow velocity of alumina in arch breaking mode is low and almost constant, and it flows like a liquid with very high viscosity. The outflow velocity of alumina in free flowing mode is higher and decays with time. This flow is truly like a liquid, and the apparent viscosity currently is close to glycerine of 0.946 Pa·s.

3.2 | Effect of pulsed aeration on stress transmission and bed structure

The pressure of grain at the bottom of a tall silo is not as high as for the equivalent column of water due to the friction between the powder and the silo wall.⁵¹ In this work, we improved the stress transmission characteristics through pulsed airflow, speculatively speaking, to make it more like the pressure characteristics of liquid. Figure 7 shows the time series of the pressure signal during discharge flow of two flow patterns. We use wavelet analysis to decompose the original pressure signal in multiple scales and give the basic pressure signal, which represents the static pressure of whole granular bed. For the arch breaking mode (see Figure 7(A)), the pressure measured in the cavity is close to zero. This is because the gas will flow through the upper arch gap, and the gas cannot be stored in the bed to form a pressure difference to increase the discharge rate. The discharge rate depends only on the behavior of arch collapse. Alumina powder has strong cohesive force and is difficult to fluidize. The gas injected into the hopper is difficult to penetrate the bed, and the gas will accumulate near the aeration vents, increasing the pressure and resulting in a peak. When the accumulated pressure exceeds the unconfined strength of the powder, the arch formed by the material will break and then be discharge. For free flowing (see Figure 7(B)), the decomposed signal represents the base pressure during discharging. It has a quadratic function relationship with time, which proves that its flow process is consistent with the pressure decay law when the liquid flows out. The outflowing particle can be pushed by the pressure transmitted from the upper material, resulting in a higher velocity.^{36,52} The flow of alumina in free flowing behaves truly like a viscous liquid.

The particles in the silo are supported to some extent by static friction with the wall, which cannot happen in a silo filled with water. But it has been found that the stick-slip behavior caused by oscillating shear can change the support of the wall to particles,⁵³ to achieve stress transmission to the bottom. Figure 8 shows the vertical stress distribution under different aeration conditions. For static packing without aeration, the measured pressure value is less than the calculated value from Janssen theory.⁵¹ This may be related to the small particle size leading to high porosity and uneven packing structure. For steady aeration, the gas can partially suspend particles to make the pressure distribution closer to the static pressure law of the liquid. Moreover, it is found that pulsed aeration can more effectively realize stress transmission than steady aeration. The vertical pressure is

FIGURE 6 (A) Snapshot of the “Arch breaking” flow pattern ($q = 20$ L/min, $f = 2$ Hz, $D = 1/2$), in which arches periodically form and collapse above the outlet of the hopper. (B) Snapshot of the “Free flowing” flow pattern ($q = 20$ L/min, $f = 10$ Hz, $D = 1/6$), in which granular materials flow smoothly out of the hopper. (C) Comparison of average apparent outflow velocity of different fluids

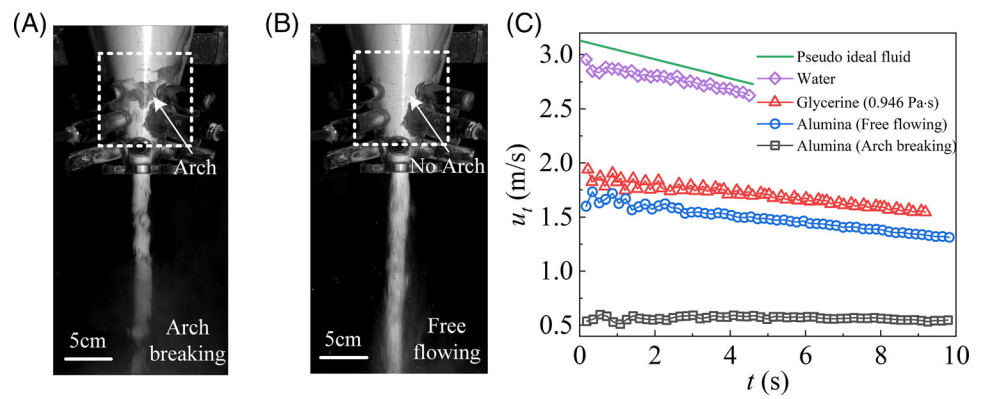
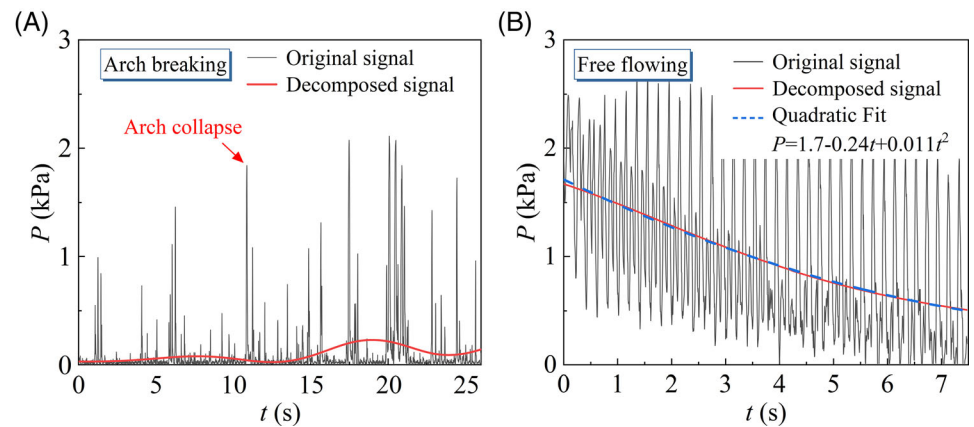


FIGURE 7 (A) Time series of pressure signal during discharge flow of “Arch breaking” (taking $q = 20$ L/min, $f = 2$ Hz, $D = 1/2$ as example). (B) Time series of pressure signal during discharge flow of “Free flowing” (taking $q = 20$ L/min, $f = 5$ Hz, $D = 1/8$ as example)



proportional with the depth of packing, and the slope is approximately the bulk density times the gravitational acceleration. Another reason for the reduction of wall friction can be explained by the air pulsation causing the breakage of the bed channel, which promotes the proper fluidization of the powder. In fact, in the fluidized powder, the wall friction is significantly reduced due to the continuous reduction of the normal stress on the wall by the particles. And in the fluidized state, the weight of the powder is completely balanced by the vertical gas-solid resistance.

When the outlet of the hopper is closed and the powder bed was aerated with pulsed airflow, the surface of the bed will oscillate up and down. This process was recorded by a high-speed camera, and the bed height change during the oscillation process can be measured with a scale ruler. The oscillation amplitude refers to the distance between the highest point and the lowest point of a movement. The results are shown in Figure 9(A). In the forced oscillation state, the effective contact support between granular packing and wall will be destroyed, which explains the elimination of Janssen effect. When the alumina powder is added to the hopper, it appears to be completely consolidated and becomes a whole. The introduced pulsed airflow will break the consolidated structure and turn it into many aggregates. The aggregate size can be measured from pictures. Using ImageJ software to calibrate the pixel size of the picture, and then use the polygon tool to outline the edge of the aggregate to obtain the projected area S . The aggregate size is defined as the

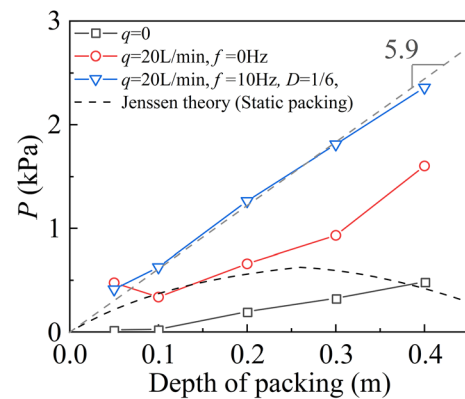


FIGURE 8 The vertical stress distributions of granular packing under different aeration conditions

diameter of a circle equal to the projected area and can be calculated from $d_a = \sqrt{\frac{4S}{\pi}}$. Figure 9(B) shows the aggregate size under different pulsed aeration conditions. The inserted image in Figure 9(B) is an example picture for aggregate size measurement. The aggregate size decreases with increasing pulse frequency and air rate. This shows that high frequency and air rate pulsed airflow can better destroy the consolidation of the bed, which means more prone to avalanches.

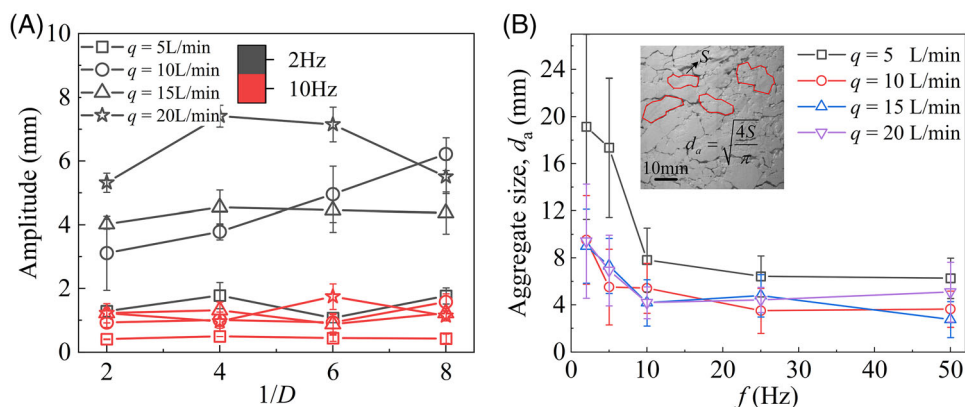


FIGURE 9 (A) Oscillating amplitude of granular bed under pulsed aeration. (B) Aggregate size under different pulsed aeration conditions. The inserted image is an example picture for aggregate size measurement

3.3 | Effect of pulsed aeration on discharge rate and aerodynamic mechanism

The discharge rate of alumina powder under different aeration conditions is shown in Figure 10. The powder is consolidated in the hopper and cannot be discharged without aeration. For steady aeration ($D = 1$), the maximum discharge rate is about 75 g/s at $q = 15$ L/min. If the average air rate is further increased, the discharge rate will no longer increase and may cause channels in the bed. According to the fluidization test, the minimum air rate is $q_{mf} = 4.24$ L/min. In the unloading experiment, even if the average gas velocity of stable ventilation is greater than q_{mf} , the whole silo cannot be fluidized well. Due to the consolidation of the powder, the gas is unevenly distributed in the bed. Steady airflow cannot overcome the problem of channels generated in the bed. For this cohesive powder, the discharge flow is

determined by the breaking of the material arch at the upper part of the hopper outlet. When the mass of powders breaking and falling from the stable arch is small, the discharge flow shows an intermittent shape, and the discharge rate is low. With the increase of the air rate, the mass of falling powders from the arch is broken increases, forming a smooth and full powder stream, the discharge rate increases.

For pulsed aeration, the discharge rate depends on the parameters of the pulsed airflow: frequency f , average air rate q and duty cycle D . When the duty cycle is lowered, the discharge rate will increase, and the higher the average air rate, the more significant the increase. The maximum discharge rate under pulsed aeration is about 250 g/s. It is close to the rate at which the pseudo ideal fluid flows. For the air rate of $q = 5$ and 10 L/min, as the duty cycle decreases, the discharge rate increase step by step. For the air rate of $q = 15$ and 20 L/min, when $D < 1/4$, the discharge rate rises sharply. This shows

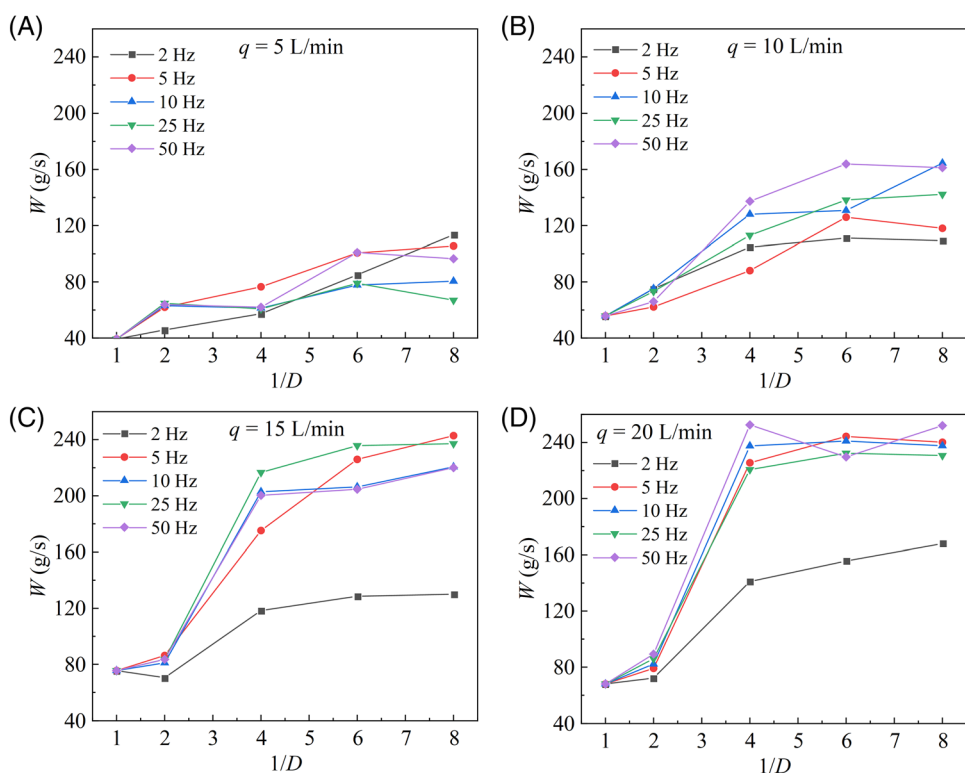


FIGURE 10 Discharge rate under different aeration conditions (A) $q = 5$ L/min, (B) $q = 10$ L/min, (C) $q = 15$ L/min, (D) $q = 20$ L/min

that the instantaneous air rate governed by duty cycle and the average air rate play a joint control effect on the flow process. The instantaneous air rate provides the impulsive force that is beneficial to break the agglomeration. Before the discharge rate reaches saturation, increasing the frequency is more conducive to strengthening the discharge rate.

The arch stress structure formed by contact friction and mechanical support between particles (or agglomerates), which will hinder the discharge flow. When the powder bed is not well fluidized, the discharge flow is unstable, and arches will form intermittently. When the collapse time of the stress structure is less than the time scale of the formation of the new stress structure, the fluidity of the particles is greatly improved.⁵⁴ The collapse time of the stress structure refers to how long the arch will break after formation. The rectangular pulsed airflow with high frequency and low duty cycle can provide stronger aerodynamics to excite collisions between particles, thereby weakening particle contact time and interparticle forces. The perturbations provided by pulsed airflow amplified by the oscillatory instability¹⁹ will trigger macroscopic avalanches. Proposed in the relevant literatures,^{24,55} the softening of particle shear contact interface stiffness can be observed under high frequency oscillating shear, which causes the decrease of apparent static friction coefficient through vibration, thus triggering macro sliding when it is far below the static yield threshold. Based on the above expression, a speculative idea can be purposed here that the oscillating force of the pulsed airflow also plays a similar role. Macroscopically, it will appear as high-intensity pulsed airflow reducing the cohesion strength of cohesive granular materials and relaxation time of stress structures. Therefore, the fluidity of the cohesive granular materials can be greatly improved, and it can be triggered to achieve a liquid-like flow transition. It is similar to the related research results of mechanical vibration excitation of granular materials.^{13,27}

Furthermore, we analyze the relationship between the discharge rate and pulse parameters. A well-known model for predicting the discharge rate of silo granular flow is Beverloo law,⁵⁶ which is suitable for flat bottomed silo. Based on this, Brown and Richards⁵⁷ proposed a correlation factor suitable for conical hopper. And Nedderman⁵⁸ proposed a pressure gradient correction relationship for fine powder considering the effect of drag force of the interstitial gas. For aerated discharge conditions in this work, the discharge rate could obey the following equation,

$$W = C\rho_b(d_0 - kd_p)^{5/2} \left(g + \frac{1}{\rho_b} \frac{dp}{dr} \right)^{1/2} \left(\frac{1 - \cos^{3/2}\alpha}{\sin^{5/2}\alpha} \right), \quad (1)$$

where W is the discharge rate; ρ_b is the bulk density; g is the gravity acceleration; d_0 is the outlet diameter of the hopper; d_p is the particle diameter (i.e., d_{32}); C and k are Beverloo empirical constants, generally providing values of 0.52 and 1.6, respectively; α is the hopper half angle; dp/dr is the pressure gradient. We can define the effective driving force of the discharge flow as.

$$g' = g + \frac{1}{\rho_b} \frac{dp}{dr}. \quad (2)$$

In the previous analysis and explanation, we believe that the oscillating force provided by the pulsed airflow breaks the consolidation of the bed and generates an effective pressure driving force. The effect of pulsed airflow can be expressed by the actual effective pressure gradient. And the effective pressure gradient dp/dr can be calculated from Equation (1). We use the kinetic energy generated by the pulsed airflow as the characterization of the pulse parameters, as follows. In a period T , the energy input to the system by a single pulsed airflow is

$$e_i \propto \frac{1}{2} m_i u_i^2 \quad (3)$$

where e_i represents the kinetic energy of a single airflow, m_i and u_i represents the mass and velocity of the single airflow, respectively. According to the definition of duty cycle, it can be written that

$$m_i \propto \frac{q}{D} \quad (4)$$

$$u_i \propto \frac{q}{D} \quad (5)$$

The total energy input to the system E_i per unit time is the energy of a single pulse air flow multiplied by the number of actions f , namely

$$E_i = e_i f \quad (6)$$

According to Equations (3)–(6), we can get

$$E_i \propto \frac{q^3 f}{D^3} \quad (7)$$

The E_i is used as a parameter to describe aerodynamic force of pulsed airflow. We can plot the relationship between the pressure gradient and the kinetic energy of the pulsed airflow as shown in Figure 11.

It can be seen from Figure 11 that the pressure gradient has both negative and positive values. E_1 is the critical energy for judging whether the effective driving force can reach gravitational

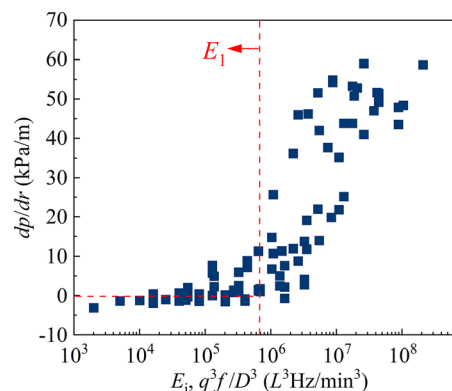


FIGURE 11 The relationship between pressure gradient and kinetic energy of pulsed airflow

acceleration. When the pressure gradient is negative ($E_i < E_1$), it indicates that the powder at the outlet is not well fluidized, and the clogging of the agglomerates at the outlet inhibits the flow. The discharge flow rate at this time is low, and the flow is also unstable. When the pressure gradient is positive ($E_i > E_1$), the aerodynamic force provided by modulated pulsed airflow can destroy the clogging at outlet and get stable discharge flow. The effective driving force increases rapidly with the input energy so that the discharge rate increases significantly.

4 | CONCLUSION

In summary, we experimentally studied the dynamic characteristics of cohesive granular materials discharged from hopper under modulated pulsed airflow. The influence of frequency, duty cycle and air rate of pulsed airflow were investigated. The results show that pulsed airflow with low duty cycle and high frequency can effectively trigger jammed cohesive granular materials stable high-flux flow. The oscillating shear provided by pulsed airflow can eliminate Janssen effect and realize stress transmission like liquid. We proposed the mechanism that the vibration provided by the pulsed airflow reduces the contact time between particles and weakens the contact between particles, thereby reducing the friction between particles and exhibiting a higher flow velocity. The use of a low duty cycle to achieve a high-strength oscillating airflow field proposed in this paper can effectively trigger the flow of fine cohesive granular materials and greatly improve its fluidity. Furthermore, we gave the scaling relationship between the pressure gradient and the pulse parameters and explained the experimental data through energy analysis. This brings more imagination to the processing and transportation of ultra-fine powders and may play a positive role in the development of related industries.

ACKNOWLEDGMENTS

The authors acknowledge financial supports from the National Natural Science Foundation of China (51876066), the National Key R&D Program of China (2018YFC0808500) and Shanghai Engineering Research Center of Coal Gasification (18DZ2283900).

AUTHOR CONTRIBUTIONS

Lizhuo Zhu: Formal analysis; investigation; methodology; visualization; writing - original draft; writing-review & editing. **Haifeng Lu:** Conceptualization; formal analysis; funding acquisition; resources; supervision; writing - original draft; writing-review & editing. **Xiaolei Guo:** Formal analysis; resources.

DATA AVAILABILITY STATEMENT

The data that support the findings of this study are available from the corresponding author upon reasonable request.

REFERENCES

- Jaeger HM, Nagel SR. Physics of the granular state. *Science*. 1992; 255(5051):1523-1531.
- Saleh K, Golshan S, Zarghami R. A review on gravity flow of free-flowing granular solids in silos – basics and practical aspects. *Chem Eng Sci*. 2018;192:1011-1035.
- Rabinovich E, Kalman H, Peterson PF. Granular material flow regime map for planar silos and hoppers. *Powder Technol*. 2021;377:597-606.
- Aranson IS, Tsimring LS. Patterns and collective behavior in granular media: theoretical concepts. *Rev Mod Phys*. 2006;78(2):641-692.
- Delannay R, Louge M, Richard P, Taberlet N, Valance A. Towards a theoretical picture of dense granular flows down inclines. *Nat Mater*. 2007;6(2):99-108.
- Mélinon P, Masenelli B, Tournus F, Perez A. Playing with carbon and silicon at the nanoscale. *Nat Mater*. 2007;6(7):479-490.
- Vo TT, Nezamabadi S, Mutabaruka P, Delenne J-Y, Radjai F. Additive rheology of complex granular flows. *Nat Commun*. 2020;11(1):1476.
- Macaulay M, Rognon P. Shear-induced diffusion in cohesive granular flows: effect of enduring clusters. *J Fluid Mech*. 2019;858:R2.
- Gans A, Pouliquen O, Nicolas M. Cohesion-controlled granular material. *Phys Rev E*. 2020;101(3):032904.
- Kou B, Cao Y, Li J, et al. Granular materials flow like complex fluids. *Nature*. 2017;551(7680):360-363.
- Pica Ciamarra M, Nicodemi M, Coniglio A. Granular packs under vertical tapping: structure evolution, grain motion, and dynamical heterogeneities. *Phys Rev E*. 2007;75(2):021303.
- Azéma E, Radjai F. Internal structure of inertial granular flows. *Phys Rev Lett*. 2014;112(7):078001.
- Gnoli A, de Arcangelis L, Giacco F, et al. Controlled viscosity in dense granular materials. *Phys Rev Lett*. 2018;120(13):138001.
- Ness C, Mari R, Cates ME. Shaken and stirred: random organization reduces viscosity and dissipation in granular suspensions. *Sci Adv*. 2018;4(3):eaar3296.
- Wortel GH, Dijkstra JA, van Hecke M. Rheology of weakly vibrated granular media. *Phys Rev E*. 2014;89(1):012202.
- Wortel G, Dauchot O, van Hecke M. Criticality in vibrated frictional flows at a finite strain rate. *Phys Rev Lett*. 2016;117(19):198002.
- Kollmer JE, Shreve T, Claussen J, et al. Migrating shear bands in shaken granular matter. *Phys Rev Lett*. 2020;125(4):048001.
- Maynar P, García de Soria MI, Brey JJ. Understanding an instability in vibrated granular monolayers. *Phys Rev E*. 2019;99(3):032903.
- Chattoraj J, Gendelman O, Pica Ciamarra M, Procaccia I. Oscillatory instabilities in frictional granular matter. *Phys Rev Lett*. 2019;123(9):098003.
- Goldman DI, Swift JB, Swinney HL. Noise, coherent fluctuations, and the onset of order in an oscillated granular fluid. *Phys Rev Lett*. 2004; 92(17):174302.
- Tsuji D, Otsuki M, Katsuragi H. Relaxation dynamics of a granular pile on a vertically vibrating plate. *Phys Rev Lett*. 2018;120(12):128001.
- Capozza R, Vanossi A, Vezzani A, Zapperi S. Suppression of friction by mechanical vibrations. *Phys Rev Lett*. 2009;103(8):085502.
- Johnson PA, Savage H, Knuth M, Gombert J, Marone C. Effects of acoustic waves on stick-slip in granular media and implications for earthquakes. *Nature*. 2008;451:57-60.
- Melosh HJ. Dynamical weakening of faults by acoustic fluidization. *Nature*. 1996;379(6566):601-606.
- Giacco F, Saggese L, de Arcangelis L, Lippiello E, Pica CM. Dynamic weakening by acoustic fluidization during stick-slip motion. *Phys Rev Lett*. 2015;115(12):128001.
- Capozza R, Vanossi A, Vezzani A, Zapperi S. Triggering frictional slip by mechanical vibrations. *Tribol Lett*. 2012;48(1):95-102.
- Clark AH, Behringer RP, Krim J. Vibration can enhance stick-slip behavior for granular friction. *Granul Matter*. 2019;21(3):55.
- Guerrero BV, Pugnali LA, Lozano C, Zuriguel I, Garcimartín A. Slow relaxation dynamics of clogs in a vibrated granular silo. *Phys Rev E*. 2018;97(4):042904.
- Janda A, Maza D, Garcimartín A, Kolb E, Lanuza J, Clément E. Unjamming a granular hopper by vibration. *EPL (Europhys Lett)*. 2009; 87(2):24002.

30. Mankoc C, Garcimartín A, Zuriguel I, Maza D, Pignaloni LA. Role of vibrations in the jamming and unjamming of grains discharging from a silo. *Phys Rev E*. 2009;80(1):011309.
31. Reichhardt C, Reichhardt CJO. Controlled fluidization, mobility, and clogging in obstacle arrays using periodic perturbations. *Phys Rev Lett*. 2018;121(6):068001.
32. Li J, Aranson IS, Kwok WK, Tsimring LS. Periodic and disordered structures in a modulated gas-driven granular layer. *Phys Rev Lett*. 2003;90(13):134301.
33. Léopoldès J, Jia X, Tourin A, Mangeney A. Triggering granular avalanches with ultrasound. *Phys Rev E*. 2020;102(4):042901.
34. Hiraiwa M, Abi Ghanem M, Wallen SP, Khanolkar A, Maznev AA, Boechler N. Complex contact-based dynamics of microsphere monolayers revealed by resonant attenuation of surface acoustic waves. *Phys Rev Lett*. 2016;116(19):198001.
35. Reichhardt CJO, Lopatina LM, Jia X, Johnson PA. Softening of stressed granular packings with resonant sound waves. *Phys Rev E*. 2015;92(2):022203.
36. Donsi G, Ferrari G, Poletto M, Russo P. Gas pressure measurements inside an aerated hopper. *Chem Eng Res Des*. 2004;82(1):72-84.
37. Barletta D, Donsi G, Ferrari G, Poletto M, Russo P. Solid flow rate prediction in silo discharge of aerated cohesive powders. *AIChE J*. 2007;53(9):2240-2253.
38. Cannavacciuolo A, Barletta D, Donsi G, Ferrari G, Poletto M. Arch-free flow in aerated silo discharge of cohesive powders. *Powder Technol*. 2009;191(3):272-279.
39. Barletta D, Russo P, Poletto M. Dynamic response of a vibrated fluidized bed of fine and cohesive powders. *Powder Technol*. 2013;237:276-285.
40. Valverde JM, Castellanos A. Effect of vibration on agglomerate particulate fluidization. *AIChE J*. 2006;52(5):1705-1714.
41. Nam CH, Pfeffer R, Dave RN, Sundaresan S. Aerated vibrofluidization of silica nanoparticles. *AIChE J*. 2004;50(8):1776-1785.
42. Barletta D, Poletto M. Aggregation phenomena in fluidization of cohesive powders assisted by mechanical vibrations. *Powder Technol*. 2012;225:93-100.
43. Zhu L, Lu H, Poletto M, Liu H, Deng Z. Hopper discharge of cohesive powders using pulsated airflow. *AIChE J*. 2020;66(7):16240.
44. Freeman RE, Cooke JR, Schneider LCR. Measuring shear properties and normal stresses generated within a rotational shear cell for consolidated and non-consolidated powders. *Powder Technol*. 2009;190(1):65-69.
45. Lu H, Guo X, Gong X, Barletta D, Poletto M. Prediction of solid discharge rates of pulverized coal from an aerated hopper. *Powder Technol*. 2015;286:645-653.
46. Lu H, Cao J, Guo X, Gong X, Fu L. Design optimization of an aerated hopper for discharge of cohesive pulverized coal. *Powder Technol*. 2019;357:186-192.
47. Lu H, Guo X, Tao S, Gong X. A further study on effect of gas type on pulverized coal discharge. *Powder Technol*. 2015;281:193-199.
48. Härtl J, Ooi JY, Rotter JM, Wojcik M, Ding S, Enstad GG. The influence of a cone-in-cone insert on flow pattern and wall pressure in a full-scale silo. *Chem Eng Res Des*. 2008;86(4):370-378.
49. Shinohara K, Idemitsu Y, Gotoh K, Tanaka T. Mechanism of gravity flow of particles from a hopper. *Ind Eng Chem Proc Des Dev*. 1968;7(3):378-383.
50. Wu X, Måløy KJ, Hansen A, Ammi M, Bideau D. Why hour glasses tick. *Phys Rev Lett*. 1993;71(9):1363-1366.
51. Nedderman RM. *Statics and Kinematics of Granular Materials*. Cambridge: Cambridge University Press; 2005.
52. de Jong JAH, Hoelen QEJMM. Cocurrent gas and particle flow during pneumatic discharge from a bunker through an orifice. *Powder Technol*. 1975;12(3):201-208.
53. Karim MY, Corwin EI. Eliminating friction with friction: 2D Janssen effect in a friction-driven system. *Phys Rev Lett*. 2014;112(18):188001.
54. Ertaş D, Halsey TC. Granular gravitational collapse and chute flow. *Europhys Lett (EPL)*. 2002;60(6):931-937.
55. Léopoldès J, Conrad G, Jia X. Onset of sliding in amorphous films triggered by high-frequency oscillatory shear. *Phys Rev Lett*. 2013;110(24):248301.
56. Beverloo WA, Leniger HA, van de Velde J. The flow of granular solids through orifices. *Chem Eng Sci*. 1961;15(3):260-269.
57. Brown RL, Richards JC. Kinematics of the flow of dry powders and bulk solids. *Rheol Acta*. 1965;4(3):153-165.
58. Nedderman RM, Tüzün U, Thorpe RB. The effect of interstitial air pressure gradients on the discharge from bins. *Powder Technol*. 1983;35(1):69-81.

How to cite this article: Zhu L, Lu H, Guo X, Liu H. Triggering flow of jammed cohesive granular materials using modulated pulsed airflow. *AIChE J*. 2022;68(1):e17411. doi: 10.1002/aic.17411